

# Theoretical analysis of the cylindrical-rectangular patch microstrip antenna in a compressible plasma

Jaswant Singh, Abhinav Dinesh, K B Sharma\* and Raj Kumar Gupta  
Department of Electrical Engineering, Malaviya Regional Engineering College  
Jaipur-302 017, India

*Received 2 March 1992, accepted 25 August 1992*

**Abstract :** Radiation from a cylindrical - rectangular patch microstrip antenna in a compressible plasma is treated as a boundary value problem. The antenna is excited by a coaxial line. The field distribution on the patch is determined by using cavity model of the analysis. A linearised hydrodynamic theory of plasma and vector wave function technique are used to deduce the expressions for electromagnetic and electroacoustic component of the far field, radiated power and radiation conductance of the antenna in compressible plasma. Numerical and graphical results are presented to illustrate the effect of plasma on radiation characteristics of the antenna in  $TM_{10}$  mode of excitation.

**Keywords :** Microstrip antenna, radiation properties, plasma

**PACS Nos. :** 41.10, Hv, 47.35 + i, 52.40 + d, 84.40 G1

## 1. Introduction

A number of applications require antennas conforming to a non-planar surface. Primary amongst these are requirements for scanning antennas on aircraft, missiles or satellite, where aerodynamic drag is reduced for a flush mounted geometry and for conformal arrays on cylindrical or hemispherical surface that provide some coverage advantage. Microstrip patch antennas are easily conformed to their mounting surface, have small volume and light weight, which make them well-suited to aerospace applications [1, 2].

An antenna mounted on space vehicle encounters high density ionized gas layer particularly during their re-entry voyage [3]. It is a well known fact that when an antenna is immersed in an ionized medium, electroacoustic waves are also generated in addition to electromagnetic waves. These electroacoustic waves change the radiation properties of the antenna to a great extent [4-6].

In this paper, a theoretical analysis of a thin cylindrical-rectangular patch microstrip antenna in compressible plasma medium is presented. The far field expressions for radiation fields, radiated power and radiation conductance in electroacoustic (EA) and electromagnetic (EM) modes are obtained. The well established hydrodynamic theory of plasma and vector

\* Present address : Department of Physics, S S Jain Subodh College, Jaipur, India

wave function technique are used to derive expressions. The results are computed and plotted for different values of refractive index of plasma parameter.

## 2. Formulation of the problem and basic equations

The plasma in which the antenna under investigation is placed is assumed as isotropic, homogeneous, lossless, and compressive medium of infinite extent. The antenna assumed to be biased to space potential so that there is no sheath formation around the antenna. Due to their relatively higher mass, the effect of ions has been neglected and plasma is assumed as a continuum of one component (electrons) fluid. Further, it is assumed that there is no static electric or magnetic field present so that the electroacoustic (EA) and electromagnetic (EM) modes are decoupled.

Considering these initial assumptions for plasma medium, and taking  $\exp(j\omega t)$  time variation, the basic equations which governs the present system are as follows [7] :

$$\nabla \times E + J\omega\mu_0 H = -M \quad (1)$$

$$\nabla \times H - J\omega\epsilon_0 E = J - n_0 e V \quad (2)$$

$$J\omega m n_0 V + n_0 e E + m v_0 \nabla n_1 = 0 \quad (3)$$

$$\nabla \cdot (n_0 V) - J\omega n_1 = 0 \quad (4)$$

where,

$J$  = electric current density,

$M$  = magnetic current density,

$m$  = electron mass,

$e$  = electron charge,

$n_0$  = average electron charge density,

$n_1$  = variation in electron charge density,

$V$  = mean electron velocity,

$v_0$  = r.m.s. thermal velocity of electron (phase velocity of EA waves).

Here, it is to be noted that in the case of incompressible plasma, the term  $m v_0^2 \nabla n_1$  occurring in eq. (3) is absent [8].

The geometry and co-ordinate system of the cylindrical-rectangular patch microstrip antenna immersed in a plasma medium are shown in Figure 1. The dimension of the straight edge is  $2b$  and that of the curved edge is  $2(a+h)\theta_1$  where ' $a$ ' is the radius of the cylinder and  $2\theta_1$  is the angle subtended by the curved edge. The thickness of the substrate is ' $h$ ' and the relative permittivity is  $\epsilon_r$ . The region between the patch and cylindrical ground plane is considered as a cavity bounded by electric wall on the top and bottom, and by magnetic wall on the side. For ' $h$ ' much smaller than wavelength, only TM modes are assumed to be excited. Using cylindrical coordinates and following the usual cavity model approximation, the electric field inside the cavity is assumed to have only  $E_\rho$  component

which is independent of 'ρ'. Source free electric field satisfies the wave equation.

$$\left( \frac{1}{\delta^2} \frac{\delta^2}{\delta\phi^2} + \frac{\delta^2}{\delta z^2} + k^2 \right) E\rho = 0. \tag{5}$$

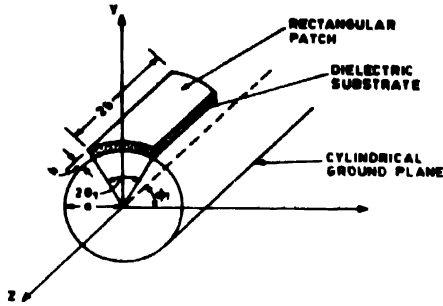


Figure 1. Geometry and coordinate system of the cylindrical-rectangular microstrip antenna in plasma

For a thin substrate satisfying  $h \ll a$  we can further assume  $\rho = a + h$  in eq. (1). Using this approximation, the eigen functions of  $E$  and eigen values of  $k$  satisfying the magnetic wall condition are given as [9],

$$E\rho = E \cos \left\{ \frac{m\pi}{2\theta_1} (\phi - \phi_1) \right\} \cos \left\{ \frac{n\pi z}{2b} \right\}. \tag{6}$$

$$k^2 = E \cos \left( \frac{m\pi}{2(a+h)\theta_1} \right)^2 + \left( \frac{n\pi}{2b} \right)^2. \tag{7}$$

The expressions for the resonant frequency is

$$f_{nm} = \frac{c}{2\sqrt{\epsilon_r}} + \left\{ \left( \frac{m}{2(a+h)\theta_1} \right)^2 + \left( \frac{n}{2b} \right)^2 \right\}^{1/2}. \tag{8}$$

Using the initial assumptions and basic equations in plasma and following the method described in [10], the general far field expressions of electric, magnetic and velocity fields in expressions of electric, magnetic and velocity fields in cylindrical coordinates are obtained as

$$E_r = \int_{-\infty}^{\infty} \left[ \sum_{n=-\infty}^{\infty} \left\{ -JL a_n \Gamma H_n'(\Gamma r) + \frac{nw\mu_0}{r} b_n H_n(\Gamma r) \right\} + \sum_{n=-\infty}^{\infty} \left\{ C_n \Gamma_p H_n'(\Gamma_p r) \right\} \left( \frac{e}{w^2 m \epsilon} \right) \exp(Jn\phi) \right] \exp(-JLz) dL, \tag{9}$$

$$E_\phi = \int_{-\infty}^{\infty} \left[ \sum_{n=-\infty}^{\infty} \left\{ \frac{nL}{r} a_n \Gamma H_n(\Gamma r) + Jw\mu_0 \Gamma b_n H_n'(\Gamma r) \right\} \right. \\ \left. - \exp(Jn\phi) + \left( \frac{Je}{w^2 m \epsilon} \right) \sum_{n=-\infty}^{\infty} \left\{ \frac{n}{r} C_n H_n(\Gamma_p r) \right\} \right] \exp(-JLz) dL, \quad (10)$$

$$E_\xi = \int_{-\infty}^{\infty} \left[ \sum_{n=-\infty}^{\infty} \left\{ \Gamma^2 a_n H_n(\Gamma r) \right\} \exp(Jn\phi) - \left( \frac{Je}{w^2 m \epsilon} \right) \right. \\ \left. \sum_{n=-\infty}^{\infty} \left\{ LC_n H_n(\Gamma_p r) \right\} \exp(Jn\phi) \right] \exp(-JLz) dL, \quad (11)$$

$$H_r = \int_{-\infty}^{\infty} \left[ \sum_{n=-\infty}^{\infty} \left\{ \frac{-nke^2}{\mu_0 w r} a_n H_n(\Gamma r) - JLb_n \Gamma b_n H_n'(\Gamma r) \right\} \exp(Jn\phi) \right] \\ \exp(-JLz) dL, \quad (12)$$

$$H_m = \int_{-\infty}^{\infty} \left[ \sum_{n=-\infty}^{\infty} \left\{ \frac{-Jke^2}{\mu_0 w} \Gamma a_n H_n'(\Gamma r) + \frac{nL}{r} b_n \Gamma H_n(\Gamma r) \right\} \exp(Jn\phi) \right] \\ \exp(-JLz) dL, \quad (13)$$

$$H_\xi = \int_{-\infty}^{\infty} \left[ \sum_{n=-\infty}^{\infty} \left\{ \Gamma^2 b_n H_n(\Gamma r) \right\} \exp(Jn\phi) \right] \exp(-JLz) dL, \quad (14)$$

and

$$V_r = \int_{-\infty}^{\infty} \left[ \left( \frac{e}{wm} \right) \sum_{n=-\infty}^{\infty} \left\{ La_n \Gamma H_n'(\Gamma r) \right\} \exp(Jn\phi) \right]$$

$$\begin{aligned}
 & + \frac{J\mu_0 e}{mr} \sum_{n=-\infty}^{\infty} \{nb_n H_n(\Gamma r)\} \exp(Jn\phi) \\
 & + \left. \frac{J\epsilon_0}{wmn_0 \epsilon} \sum_{n=-\infty}^{\infty} \{C_n \Gamma_p H'_n(\Gamma_p r) \exp(Jn\phi)\} \right] \exp(-JLz) dL. \quad (15)
 \end{aligned}$$

In these expressions,  $a_n$ ,  $b_n$  and  $c_n$  are arbitrary coefficients,  $H_n(z)$  and  $H'_n(z)$  are the Hankel function of second kind and its derivative of order  $n$  and argument ( $z$ ) respectively. The functions  $\Gamma$  and  $\Gamma_p$  are given as

$$\Gamma = (ke^2 - L^2), \quad (16)$$

$$\Gamma_p = (kp^2 - L^2), \quad (17)$$

where  $L = ke \cos\theta$  or  $kp \cos\theta$ ,  $ke$  and  $kp$  are propagation constant for EM and EA modes respectively and defined as  $ke = k_0 A$ ,  $kp = (c/v_0) ke$  and  $A = (1 - \omega p^2/\omega^2)^{1/2}$

where,  $k_0$  is free space propagation constant,  $A$  is refractive index of plasma medium (plasma parameter),  $\omega p$  is angular plasma frequency.

### 3. Evaluation of radiation field

To determine the coefficients ( $a_n$ ,  $b_n$  and  $c_n$ ), we compare the tangential field computed from above expressions at  $r = a$  with the assumed field on the surface of the cylinder and putting acoustic velocity component ( $V_r$ ) equal to zero at the surface of the cylinder. The values  $a_n$ ,  $b_n$  and  $c_n$  are obtained as

$$a_n = \frac{B_{1e} C_{3e} \bar{E}_{\phi e} + (B_{2e} C_{1e} - B_{1e} C_{2e}) \bar{E}_{ze}}{2\pi [B_{1e} (A_{2e} C_{3e} - A_{3e} C_{2e}) - B_{2e} (A_{1e} C_{3e} - A_{3e} C_{1e})]}, \quad (18)$$

$$b_n = \frac{(A_{3e} C_{1e} - A_{1e} C_{3e}) \bar{E}_{\phi e} + (A_{1e} C_{2e} - A_{2e} C_{1e}) \bar{E}_{ze}}{2\pi [B_{1e} (A_{2e} C_{3e} - A_{3e} C_{2e}) - B_{2e} (A_{1e} C_{3e} - A_{3e} C_{1e})]}, \quad (19)$$

$$c_n = \frac{1}{C_{3p}} \left\{ \frac{E_{zp}}{2\pi} - \frac{B_{1p} C_{3p} A_{3p} \bar{E}_{\phi p} + A_{3p} (B_{2p} C_{1p} - B_{1p} C_{2p}) \bar{E}_{zp}}{2\pi [B_{1p} (A_{2p} C_{3p} - A_{3p} C_{2p}) - B_{2p} (A_{1p} C_{3p} - A_{3p} C_{1p})]} \right\}, \quad (20)$$

where  $A_{1e}$ ,  $B_{1e}$ ,  $C_{2e}$  etc. are functions of  $\theta$  and  $\phi$  and values of these are given in appendix A.  $\bar{E}_{\phi e}$ ,  $\bar{E}_{ze}$  etc. are Fourier transforms of the aperture fields. The values of these are finally obtained as

$$\bar{E}_z(n, L) = \frac{E_0 b}{2\pi} [1 - (-1)^n \exp(-2jbL)] I_1, \quad (21)$$

$$\bar{E}_{\phi}(n, L) = \frac{E_0 b}{2\pi a} [1 - (-1)^m \exp(-2jn\theta_1)] I_2, \quad (22)$$

where, 
$$I_1 = \int_{-2b}^0 \cos\left(\frac{m\pi\phi}{2\theta_1}\right) \exp(-In\phi) d\phi, \quad (23)$$

$$I_2 = \sum_0^{2\theta} \cos\left(\frac{n\pi z}{2b}\right) \exp(-ILz) dz. \quad (24)$$

The values of  $\bar{E}_z e$  or  $\bar{E}_{zp}$  can be obtained by putting  $L = ke \cos\theta$  or  $L = kp \cos\theta$  respectively in eq. (21). Similarly the values of  $E_{\phi e}$  or  $E_{\phi p}$  can be obtained from eq. (22).

Using these values of  $a_n$ ,  $b_n$  and  $c_n$ , making suitable manipulations and transforming the expressions from cylindrical to spherical coordinates, the EM mode and EA mode far zone fields in plasma medium are obtained as follows :

For EM mode .

$$E_{\theta} = \frac{-2j}{r_0} (ke^2 \sin\theta) \exp(-jker_0) \sum_{n=-\infty}^{\infty} a_n j^n \exp(jn\phi), \quad (25)$$

$$E_{\phi} = \frac{-2jw\mu_0}{r_0} (ke \sin\theta) \exp(-jker_0) \sum_{n=-\infty}^{\infty} b_n j^n \exp(jn\phi), \quad (26)$$

$$H_{\theta} = \frac{-2j}{r_0} (ke^2 \sin\theta) \exp(-jker_0) \sum_{n=-\infty}^{\infty} b_n j^n \exp(jn\phi), \quad (27)$$

$$E_{\phi} = \frac{-2j}{w\mu_0 r_0} (ke^2 \sin\theta) \exp(-jker_0) \sum_{n=-\infty}^{\infty} a_n j^n \exp(jn\phi), \quad (28)$$

For EA mode .

$$E_{r\theta} = \frac{2ekp}{w^2 m \epsilon r_0} \exp(-jK_p r_0) \sum_{n=-\infty}^{\infty} C_n j^n \exp(jn\phi). \quad (29)$$

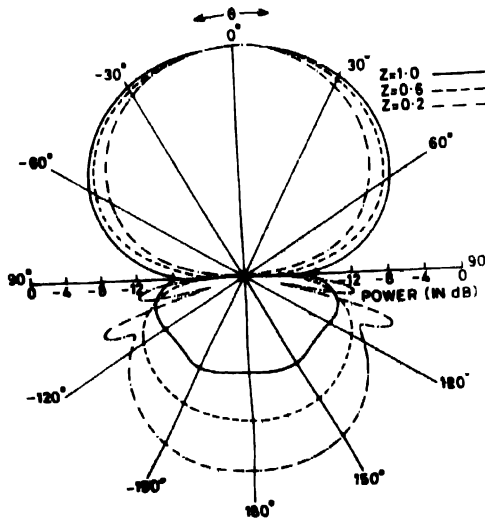


Figure 2. Variation of EM mode field pattern factor with plasma parameter in  $\theta = 90^\circ$  plane.

Using eqs. (25) to (29), the power pattern factors for EM and EA mode computed for  $TM_{10}$  mode of the excitation. The computations are done for a case taking resonant frequency 10 GHz, dielectric constant of substrate ( $\epsilon_r$ ) = 2.5, thickness of the substrate ( $h$ ) = 0.159 cm and radius of cylinder ( $a$ ) = 1.12 cm.

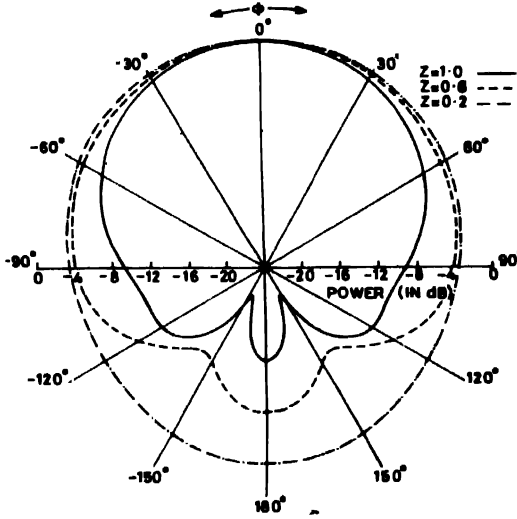


Figure 3. Variation of EM mode field pattern factor with plasma parameter in  $\phi = 90^\circ$  plane.

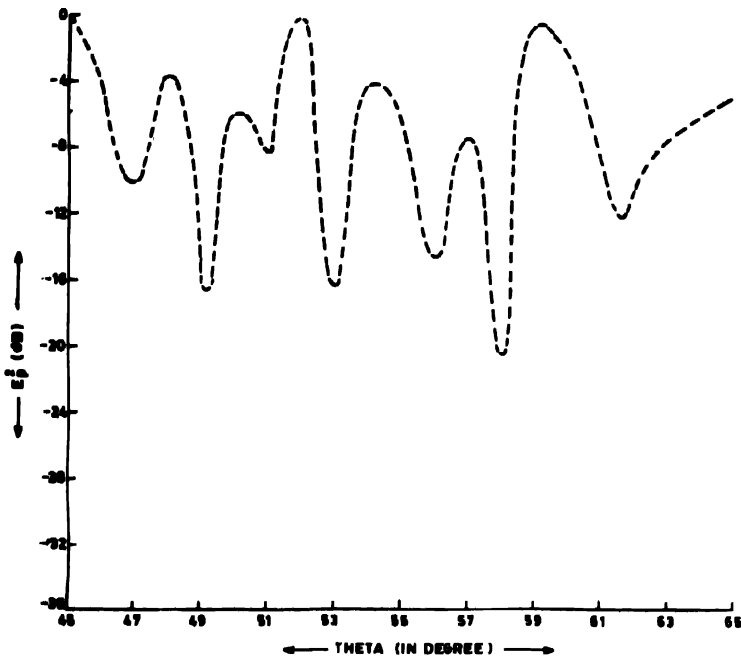


Figure 4. Electroacoustic mode field patterns in  $\phi = 90^\circ$  plane.

The pattern factor in EM mode is computed for three values of refractive index of plasma (plasma parameter) i.e.  $A = 1.0$  (free space,  $A = 0.6$  (plasma) and  $A = 0.2$  (plasma). The results are plotted in Figures 2 and 3 for  $\theta = 90^\circ$  and  $\phi = 90^\circ$  planes.

The electroacoustic mode pattern factor is computed for  $A = 0.6$  and  $\phi = 90^\circ$ . A representative EA mode pattern are plotted for  $20^\circ$  interval ( $45^\circ$  to  $65^\circ$ ) in Figure 4.

#### 4. Radiated power and radiation conductance

The radiated power through upper half-space is found by integrating the complex Poynting vector over a large hemispheric surface. Thus radiated power in EM mode is defined as [5]

$$P_e = \frac{A}{2Z_0} \int_0^{\pi/2} \int_0^{2\pi} |E_\theta^2 + E_\phi^2| r_0^2 \sin\theta d\theta d\phi, \quad (30)$$

where  $Z_0$  is free-space impedance.

Similarly the radiated power in EA mode is defined as [5]

$$P_p = \frac{A}{1-A^2} \frac{v_0}{c} \frac{1}{Z_0} \int_0^{\pi/2} \int_0^{2\pi} (E_{r_0})^2 r_0^2 \sin\theta d\theta d\phi. \quad (31)$$

Putting the values of  $E_\theta$ ,  $E_\phi$  and  $E_{r_0}$  in eqs. (30) and (31), the values of  $P_e$  and  $P_p$  are computed using Simpson's rule of integration for different values of plasma parameter.

The radiation conductance in EM and EA modes are defined as

$$G_e = \frac{2P_e}{V_0^2} \quad (32)$$

$$\text{and } G_p = \frac{2P_p}{V_0^2} \quad (33)$$

where  $V_0$  is the edge voltage.

Using the values of  $P_e$  and  $P_p$ , the values of  $G_e$  and  $G_p$  are computed for different values of plasma parameter. The results are plotted in Figure 5.

#### 5. Results and discussions

As shown in Figures 2 and 3 and Table 1, a considerable effect of plasma is noted on the beam width of the cylindrical-rectangular microstrip antenna. The variation in beam width with plasma parameter is not uniform in  $\phi = 90^\circ$  and  $\theta = 90^\circ$  planes. In  $\theta = 90^\circ$  plane the beam width is increased as the plasma parameter is decreased. On the other hand, it is decreased in  $\phi = 90^\circ$  plane as the plasma parameter is decreased. Further, greater variation in the beam width is noted in case of  $\theta = 90^\circ$  plane.



A different performance of the antenna is also for the radiation in end-fire direction in  $\phi = 90^\circ$  and  $\theta = 90^\circ$  planes. A lower power level of the antenna in the end-fire direction is

Table 1. Main features of the EM mode radiation patterns.

Plasma parameter	Beam width		Reduced power level in end fire direction (In dB)		Back lobe level (In dB)	
	$\phi = 90^\circ$	$\theta = 90^\circ$	$\phi = 90^\circ$	$\theta = 90^\circ$	$\phi = 90^\circ$	$\theta = 90^\circ$
1.0	100°	96°	- 16.8	- 9.2	- 14.0	- 14.1
0.6	96°	140°	- 20.4	- 4.2	- 9.0	- 8.9
0.2	80°	160°	- 27.5	- 3.5	- 3.4	- 3.4

noted in  $\phi = 90^\circ$  plane, which is further reduced as the plasma parameter is decreased. While in  $\theta = 90^\circ$  plane the better radiation performance in the end-fire direction is further improved as the plasma parameter is decreased.

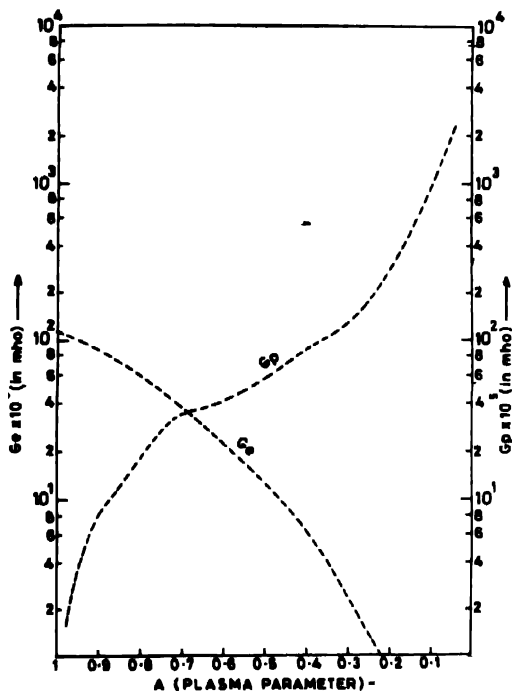


Figure 5. Variation of radiation conductance with plasma parameter in EM and EA modes.

The back lobe level of the antenna is almost same in both planes. Further, it is increased in both planes as the plasma parameter is decreased.

The EA mode pattern of the antenna shows a large number of lobes in a short angle range. A similar behaviour of the patterns is noted for other angle ranges, hence a representative pattern is plotted in Figure 4.

The radiation conductance of the antenna is varied differently with plasma parameter in EM and EA modes. In the EM mode the radiation conductance is decreased while in EA

mode it is increased for lower values of plasma parameter. The conductance in both modes have same values approximately at  $A = 0.68$ .

The above discussed changes in the radiation characteristics of the antenna in plasma medium are observed due to the different propagation constants in different conditions.

In EM mode patterns, the propagation constant depends on the plasma frequency which depends on plasma density. Therefore, for different plasma frequencies, different radiation patterns (beam width, side lobe, back lobe, etc.) are obtained.

In EA mode pattern, the large number of lobes is obtained. As indicated by Freeston and Gupta [11], this is due to the factor  $c/v_o$  ( $k_p = c/v_o k_e$ ) which occurred in the arguments of Hankel's functions of second kind and their derivatives in the expression for  $c_n$  in eq. (16).

In case of radiation resistance, as the plasma frequency reaches closer to source frequency, more power goes in EM mode. That is why the power radiated in EM mode reduces as refractive index of plasma is reduced. This ultimately results in decrease in radiation conductance in EM mode and increase in radiation conductance in EA mode when the refractive index decreases.

## 6. Conclusions

The radiation properties of the cylindrical-rectangular patch microstrip antenna are predicted in the plasma medium. A significant effect of plasma is noted on radiation patterns, radiated power, and radiation conductance of the antenna. The radiation conductance of the antenna in EM mode is decreased due to the fact that as the plasma frequency increases more power goes in the EA mode.

Finally, the study is very useful for aerospace applications as this antenna can be easily flush mounted on the cylindrical surfaces of the aerospace vehicles.

## Acknowledgment

The authors are indebted to Indian Space Research Organisation, Bangalore for providing the project grant and senior research fellowships to JS and AD. The authors also gratefully acknowledge the useful suggestions given by Dr C L Arora, Head, Department of Physics, MREC, Jaipur and Dr V K Saxena, Department of Physics, University of Rajasthan, Jaipur.

## References

- [1] K R Carver and J W Mink 1981 *IEEE Trans AP-29* 1
- [2] R E Munson 1974 *IEEE Trans AP-22* 74
- [3] R L Fante 1967 *Radio Sci* 2 87
- [4] K M Chen 1964 *Proc IEE* 111 1668
- [5] I L Freeston and R K Gupta 1978 *Proc IEE* 118 633
- [6] Jaswant Singh and R K Gupta 1991 *J Inst Elect and Telecommun. Engg.* 37 285
- [7] J Carlin and R Mitra 1967 *Radio Sci* 2 1327
- [8] K M Chen 1965 *Radio Sci* 69D 243
- [9] C M Krowne 1983 *IEEE Trans AP-31* 194
- [10] J R Wait 1966 *IEEE Trans AP-14* 360
- [11] R K Gupta and I L Freeston 1973 *Int. J. Electronics* 34 545

**Appendix A**

$$A_1 = \frac{eL}{wm} \Gamma H_n(\Gamma a) \quad (\text{A-1})$$

$$B_1 = \frac{j\epsilon\mu_0}{am} n H_n(\Gamma a) \quad (\text{A-2})$$

$$C_1 = \frac{j\epsilon_0}{wm\eta_0\epsilon} \Gamma_p H_n'(\Gamma_p a) \quad (\text{A-3})$$

$$A_2 = \frac{nL}{a} \Gamma H_n(\Gamma a) \quad (\text{A-4})$$

$$B_2 = jw\mu_0 \Gamma H_n'(\Gamma a) \quad (\text{A-5})$$

$$C_2 = \frac{j\epsilon n}{w^2 m a \epsilon} H_n(\Gamma_p a) \quad (\text{A-6})$$

$$A_3 = \Gamma^2 H_n(\Gamma a) \quad (\text{A-7})$$

$$B_3 = 0 \quad (\text{A-8})$$

$$C_3 = \frac{-j\epsilon L}{w^2 m \epsilon} H_n(\Gamma_p a) \quad (\text{A-9})$$